Journal of Operation and Automation in Power Engineering

vol. XX, no. XX, Dec. 2022, Pages: XXXX (Proofed)

http://joape.uma.ac.ir

An Application of the Genetic Algorithm Optimization to Voltage and Reactive Power Control in the Distribution Systems

A.S. Altuma[1], R. Khalid[2], A.I. Alanssari[3], H.A. Ali[4], Y.S. Mezaal[5], K. Al-Majdi[6], T. Alawsi[7]

[1] *University of Kerbala/ College of Engineering/ Department of Electrical and Electronics Engineering/Iraq.*
[2] *Medical technical college; Al-Farahidi University, Baghdad , Iraq.*
[3] *Al-Nisour University College/Iraq.*
[4] *Department of Medical Laboratory Technics, Al-Zahrawi University College, Karbala, Iraq.*
[5] *Al-Esraa University College, Baghdad, Iraq*
[6] *Department of biomedical engineering/ Ashur University College/Baghdad/ Iraq.*
[7] *Scientific Research Center, Al-Ayen University, Thi-Qar, Iraq.*

Abstract— *Insufficient synchronization between the operational efficiency of capacitors and tap-changer transformers in regulating voltage presents a fundamental challenge in distribution networks, which in turn hinders the control performance. This challenge is caused by the inability of these two components to synchronize their respective operations properly. In this study, a novel control strategy is presented with the objective of achieving synchronization in the functioning of capacitors and tap transformers. Depending on the load change, various devices can be used to control the distribution network voltage. On Load Tap Changers (OLTCs) and Capacitor Banks (CBs) respond slowly to voltage changes. If the voltage changes rapidly, such devices are useless and should be avoided. Keying may shorten lifespan. This study investigated a new optimal control mechanism for coordinating tap transformers and capacitors. The optimization of tap trans- and capacitor-stage operation through the use of a Genetic Algorithm (GA) results in the reduction of superfluous switching. The limits for Point of Common Coupling (PCC) bus voltage and power factor are 0.94 and 1.02 per unit, respectively. The secondary control stage regulates the voltage of the feeder bus within the range of 0.95 to 1.05 per unit. Following the second-stage regulation of the terminal buses in the N network feeder, the third stage governs the PCC bus voltage. To prevent an infinite control loop, the voltage of the PCC bus is regulated within the range of 0.95 to 1.05 per unit (PU). These findings indicate that the optimization model is capable of achieving maximum efficiency in controlling the voltage of the distribution network. In the interim, this optimization technique produces outcomes of greater accuracy, as evidenced by a voltage value that remains consistently close to unity [Root Mean Square Error (RMSE) = 0.85] across a broad spectrum of network-loading scenarios.*

Keywords—Optimization, Genetic Algorithm, Voltage Control, Capacitor.

NOMENCLATURE

Abbreviations

CB	Capacitor Banks
DG	Distributed Generation
GA	Genetic Algorithm
MPC	Model Predictive Control
MSO	Moth Search Optimization
OLTC	On Load Tap Changers
PCC	Point of Common Coupling
PU	Per Unit
RMSE	Root Mean Square Error
VR	Voltage Regulators

1. INTRODUCTION

Capacitive voltage transformers are used to transform high voltages into signals suitable for protection and control systems in high-pressure and high-pressure systems [1–3]. Utilizing capacitor voltage transformers in high-pressure systems significantly reduces the cost of voltage conversion [4, 5]. However, the transient behavior of capacitor voltage transformers during short circuits is inappropriate, owing to their structural characteristics [6, 7]. This transient behavior causes protection relays, particularly distance relays, to operate improperly or delay sending the disconnection command [8]. Owing to the energy storage elements of the inductor and capacitors of the capacitive voltage transformer and the nonlinear characteristics of the transformer core, the output voltage of capacitive voltage transformers does not exactly follow the input voltage when the voltage drops drastically owing to a fault, and there is a transient period in the operation of capacitive voltage transformers [9, 10]. The transient performance of the capacitor voltage transformers diminishes the primary component of the error voltage. This reduction in the voltage's primary component decreases the calculated impedance [11]. If the reduction in the main voltage is sufficient, the distance relay zone functions incorrectly, and it operates when the fault is located outside the protection zone [12]. Considering the escalating international sanctions imposed on the energy sector of Middle Eastern nations, exemplified by the sanctions imposed on Iraq in the 1990s and Iran in the 2010s, it is imperative to explore viable measures to safeguard energy production and distribution systems [13–15].

It is evident that any factor that introduces an error in

Received: 30 Mar. 2023
Revised: 02 Aug. 2023
Accepted: 27 Aug. 2023
*Corresponding author:
E-mail: ahmedselmanaltuma@gmail.com (A.S. Altuma)
DOI: 10.22098/joape.2023.12614.1955
Research Paper

the measured current and voltage will result in the inaccurate functioning of the distance relay [16]. Changes in the operating conditions of the network, changes in the network structure, conditions of the occurrence of errors, and errors related to protective transformers are among the factors that cause errors in the current and voltage seen by the remote relay and can lead to incorrect operation of the relay [17].

To address this issue, a percentage of the impedance of the lines was conservatively chosen in the traditional method of setting the distance relay so that there was no interference in the operation of the relays in the event of an out-of-line error. Some studies have suggested adaptive protection by adjusting the distance relay to solve this problem. Research on distance relay settings has been conducted in a comparative manner under the conditions of load changes, power fluctuations, and fault resistance [18–21]. Several types of performance characteristics have been proposed in relays for different system conditions to solve the error caused by dynamic loads [22]. The main issue with these two solutions is their high prices. Furthermore, some uncertainties, such as the size of the fault resistance and the accuracy of the protective transformers, cannot be considered.

Reducing the zone range of a relay is a common solution to the problem of distance relay over range, caused by the transient behavior of capacitor voltage transformers. Another method is to create a delay in the operation of the protection zone of a distance relay. During the transient states of the capacitor voltage transformers, this delay prevents the relay from operating. This method lengthens the time required to rectify near-relay errors [23]. Hou and Roberts [24] presented a neural-network-based algorithm to eliminate the effect of the transient behavior of capacitor voltage transformers. Using inverse neural networks, the transfer function of a capacitor voltage transformer was modeled. A method based on the use of a nonreversible digital filter in a distance relay to eliminate the transient behavior of the capacitor voltage transformer was presented by Siguerdidjane et al [25]. Khorashadi-Zadeh [26], presented a neural-network-based algorithm to eliminate the effect of the transient behavior of capacitor voltage transformers. Using inverse neural networks, the transfer function of a capacitor voltage transformer was modeled. Yousefi et al. [27] presented a method for managing reactive power in a distribution system. The method under consideration places emphasis on the phenomenon of voltage rise in distribution systems that are outfitted with a significant quantity of photovoltaic units. Go et al. [28] presents a two-step method for controlling devices such as On Load Tap Changer (OLTC) and Capacitor Banks (CBs). Rui et al. [29] examined OLTC and CB for voltage and reactive power regulation. A distribution network voltage and reactive power optimization model is created first. This model is relaxed to MISOCP from the branch power flow equation. Huang et al. [30] provided online reactive power and voltage control using a hybrid mechanism-data model and source-load uncertainty. An offline deterministic-stochastic optimization technique educated the model. Source-load uncertainty affects reactive power optimization. The hybrid-driven solution meets real-time voltage control requirements and is more versatile. Considering device action costs, model predictive control (MPC) is suggested for rolling optimization, the upgraded IEEE-33 bus assessment mechanism validates the suggested approach. The Moth Search Optimization (MSO) technique is used by Pouladi et al. [31] to solve the problem of renewable resource accumulation in the distribution network. Using this technique, the performance of OLTC and renewable resources is coordinated, resulting in cost and voltage deviation reduction. Singh et al. [32] presented a voltage control method in which each bus can inject active and reactive power into the network and improve network voltage by measuring the local voltage. Local voltage measurement is used in this method. A non-linear programming model is presented by Magnússon et al. [33] with the goal of reducing the number of unsupplied loads and improving equipment switching performance by coordinating renewable resources and voltage control equipment. Vargas et al. [34] presented a new method for optimally controlling between OLTC and network capacitors, with the bus voltage value set between 0.94 and 1.05 PU. There is no connection between the OLTC and the grid capacitors in this method. Time delay has also been used to reduce the number of OLTC switches and network capacitors. In their study, Xu et al. [35] introduced a two-step approach for the synchronization of tap changer, capacitor banks, and Distributed Generation (DG). This approach involved the utilization of two distinct controllers to facilitate effective communication. In their study, Mehmood et al. [36] introduced a methodology for the identification of a set of control variables, namely DG, OLTC, and CBs, that exhibit the greatest impact on voltage control within the distribution network. Alzaareer et al. [37] proposed a control structure consisting of seventeen zones to effectively regulate the integration of voltage and reactive power. Experimental scenarios have been determined for each area, wherein the state of the capacitor or tap transformer is altered. The primary issue with this method is that the network operates solely on binary values, represented as zeros and ones, as demonstrated by these scenarios.

In this study, we delve into the research behind simultaneously optimizing the network's voltage controls and power factor controls to achieve optimal performance. To accomplish this, the operation of the tap transformer and capacitor is presented in such a way that switching is not performed unless it is absolutely necessary to do so. Here, a Genetic Algorithm (GA) was used to optimize the states of the OLTC and capacitor and automate the process. This led to more accurate control of the network voltage and power factor (within the ranges of 0.98 to 1.02 for the former and 0.95 for the latter, respectively).

2. MATERIALS AND METHODS

General scenarios for coordinated voltage and reactive power regulation can be considered using a capacitor and a transformer. These scenarios include capacitor input, capacitor output, tap transformer increase, and tap transformer decrease. If the voltage and power factor are such that the established area is not in the target area, the scenario for that area should be such that changing the position of the capacitor or tap transformer causes the voltage and power factor to approach or go to the target area. The target range of voltage and power factor values is limited.

2.1. Controller structure

The first control stage's goal is to control the voltage and power factor of the Point of Common Coupling (PCC) bus using the tap transformer and all capacitors. According to the PCC bus voltage and power factor values are also classified into two levels. It should be noted that the permissible limits for PCC bus voltage and power factor are 0.94 and 1.02 PU. The final bus voltage of the feeders is controlled within the range of 0.95 to 1.05 PU in the second control stage. After finishing the voltage control of the terminal buses in the N network feeder, which is done in the second stage, the third control stage starts, in which the PCC bus voltage is controlled again. In order to avoid creating an endless control loop at this stage, the value of the PCC bus voltage is controlled within the range of 0.95 to 1.05 PU. The presented method formulates reactive power allocation as an extension of Newton-Raphson propagation method. The most famous method for solving nonlinear equations is Newton-Raphson method. In this method, we start with an initial estimation. The Taylor series were written for the equations and omit the high-order terms. The result of this is the transformation of the nonlinear system into a linear system as follows:

$$\begin{bmatrix} \Delta\theta \\ \Delta|V| \end{bmatrix} = -J^{-1} \begin{bmatrix} \Delta P \\ \Delta Q \end{bmatrix} \tag{1}$$

where, ΔP and ΔQ are calculated from the (2):

$$\Delta P_i = -P_i + \sum_{k=1}^{N} |V_i|\,|V_k|\,(G_{ik}\cos\theta_{ik} + B_{ik}\sin\theta_{ik}),$$
$$\Delta Q_i = -Q_i + \sum_{k=1}^{N} |V_i|\,|V_k|\,(G_{ik}\sin\theta_{ik} - B_{ik}\cos\theta_{ik}). \quad (2)$$

and the Jacobian matrix is calculated from the (3):

$$J = \begin{bmatrix} H & N \\ J & L \end{bmatrix} = \begin{bmatrix} \frac{\partial \Delta P}{\partial \theta} & \frac{\partial \Delta P}{\partial |V|} \\ \frac{\partial \Delta Q}{\partial \theta} & \frac{\partial \Delta Q}{\partial |V|} \end{bmatrix}. \quad (3)$$

The values of voltage and angle for repetition are calculated according to the (4):

$$\theta^{m+1} = \theta^m + \Delta\theta$$
$$|V|^{m+1} = |V|^m + \Delta|V|. \quad (4)$$

These repetitions continue until ΔP and ΔQ become smaller.

In this method, the number of iterations required to converge to the solution is minimized. The frequency of iterations is not contingent upon the quantity of supervisors, and the rate of attaining the solution is considerable. The stability and convergence of this method are generally reliable, resulting in more precise solutions. The matrix that is the reciprocal of the Jacobian matrix is commonly referred to as the sensitivity matrix. The linear function of the network's constraints can be expressed in terms of variables by utilizing the elements in the sensitivity matrix. The proposed method's overview process is depicted in Fig. 1, and it is specifically designed for a network comprising N feeders. The optimization model delineates a novel scenario for the tap transformer and capacitor in each of the three stages, contingent upon the control variable values and the predefined scenarios for the proposed structure's areas. Subsequently, the capacitor or tap transformer's updated state is automatically imposed onto them, leading to the optimization of voltage value and power factor.

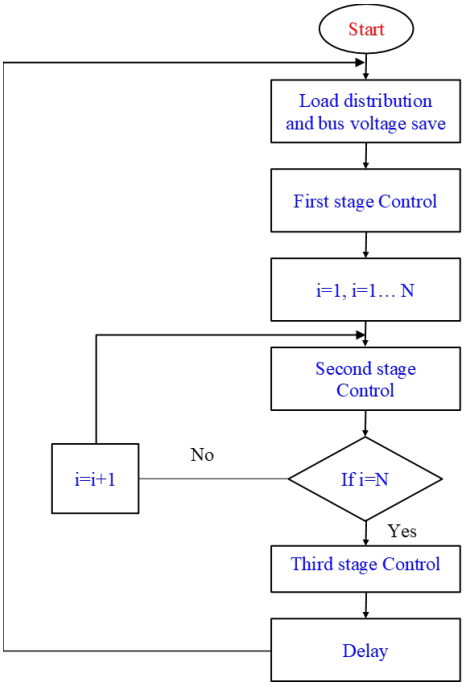

Fig. 1. Proposed method process.

2.2. Genetic algorithm

A number of optimization algorithms have been suggested in the literature as potential solutions for addressing the restoration problem in distribution systems [38–40]. An alternative strategy for addressing an optimization problem involves employing precise techniques to directly solve the mathematical formulation of the problem. The basis of the work of the GA is working on chromosomes and correcting the design and variables (genes) at each stage based on the calculated objective function corresponding to each chromosome. This indicates that the variable and the design's fundamental parameters, each of which is known as a gene, form a set known as a chromosome. The primary characteristic of chromosomes is their one-to-one relationship. Consequently, a number can be assigned to each chromosome, which corresponds to the objective function that was calculated for it. Each gene appears in the chromosome in a slow manner, meaning that the parameters or variables are encoded and placed in the chromosome according to a specific method [41]. Therefore, one bit is assigned to this chromosomal parameter. Therefore, according to each gene, it also consists of a number of adjacent bits, each of which can be either zero or one, and the adjacent bits in the form Coded constitute the corresponding parameter. A consideration in allocating the number of bits to each gene and its coding, and another advantage of the GA over other optimization methods, is that the problem can be constrained by selecting the number of bits and coding without the need for a priori knowledge. Enter the inequalities caused by the feud in various parts of the design and apply the design to the entire problem [42].

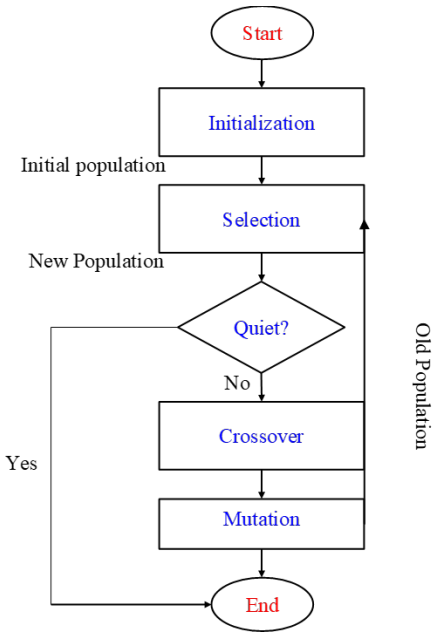

Fig. 2. GA flowchart.

Identifying and forming chromosomes is the initial step in implementing the GA. The subsequent actions are as follows: Selecting two chromosomes from the existing chromosome population at random with Paying close attention to the objective function that has been calculated for them; Generation of an offspring chromosome from two selected chromosomes using displacement operators and mutation; Executing the new chromosome procedure; Calculate the objective function for the newly designed transformer based on the new chromosome; Compare the objective function and the control criterion in order to reach the optimal point; if the optimal point is not reached, include this chromosome in the initial population. After applying these changes, the performance of the algorithm was repeatedly evaluated using data obtained from various experiments. In some cases, convergence was achieved while executing the program with random initial values for the parameter values, while in others, convergence was not achieved. In this instance, convergence was

achieved in all cases, and in the worst case, parameters were set after approximately 2,000 iterations and three hours of execution time.

The objective function (F), presented in (5), reduces the number of fundamental loops while minimizing the nonrestored demand.

$$\begin{aligned}\text{minimize}\quad F = &\sum_{i\in\Gamma_N^D|S_i\notin\Gamma_S^F} c_i^{LS} S_i^D y_i + \sum_{ij\in\Gamma_B^C} c_{ij}^{SW}(1-w_{ij}) \\ &+ \sum_{ij\in\Gamma_B^O} c_{ij}^{SW} w_{ij} + \sum_{i\in\Gamma_N^{CB}} c_i^{CB}\hat{n}_i^{CB} \\ &+ \sum_{i\in\Gamma_N^{DG}} (c_i^{DGp}\hat{P}_i^{DG} + c_i^{DGq}\hat{Q}_i^{DG}) \\ &+ \sum_{ij\in\Gamma_B^{TC}} c_{ij}^{TC}\hat{\delta}_{ij}^{TC} \\ +c^{LP}\times&\left(+\sum_{ij\in\Gamma_B} w_{ij} - |\Gamma_N| + |\Gamma_N^{TS}| + |\Gamma_N^{AS}|\right)\end{aligned} \tag{5}$$

where, c_i^{LS}, $c_i j^{SW}$, c^{LP}, c_i^{CB}, c_{ij}^{TC}, c_i^{DGp}, and c_i^{DGq} are cost of the out-of-service load, line switching, loop formation, modifying the status of a CB, modifying the status of a VR/OLTC, and changing the active/reactive output of a DG respectively. The initial term quantifies the total nonrestored burden without taking into account the demand at the faulty section. The second and third calculations impose penalties on the operations of the normally closed and normally open switches, respectively. The fourth penalty pertains to the alteration of the operational status of the CBs. In a similar vein, the fifth term imposes penalties on the adjustments made to the active and reactive power distributions of DGs. The sixth term imposes penalties for modifications made to the trigger's location on voltage regulators (VRs) and OLTCs. The number of fundamental loops in a system is determined by the final term. The convergence curve of genetic algorithm for peak load is shown in Fig. 3.

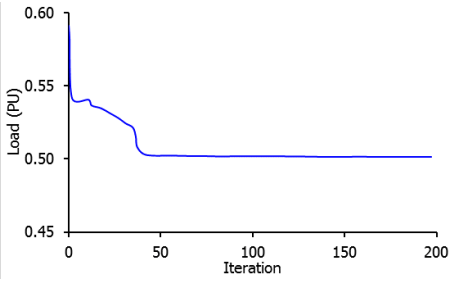

Fig. 3. Convergence curve.

3. RESULTS AND DISCUSSION

In this section, the proposed method presented in the third section is implemented on the studied network. The simulations have been done with MATLAB tool. Based on the network information provided by Vargas et al. [34], this study's network consists of a 70.10 kV transformer with 32 tap positions. There is a capacitor bank with a total capacity of 4 MW on the PCC bus and 2.8 MW on each of the feeders. Table 1 illustrates the variations observed in the post tap when the DGs are categorized as controllable and non-controllable. Based on the findings, it is observed that the magnitude of tap changes is comparatively lower when the DGs are controlled, as opposed to when they are uncontrolled. However, it should be noted that the uncontrolled scenario is more common in practical applications due to the constraints associated with keying.

Table 1. Tap variation in system with controllable and non-controllabl.

Hour	No control	With control	Hour	No control	With control
1	0	0	13	6	0
2	0	0	14	6	0
3	0	0	15	0	0
4	0	0	16	0	0
5	0	0	17	8	0
6	4	0	18	8	1
7	6	0	19	8	1
8	6	0	20	8	1
9	6	0	21	6	1
10	6	0	22	5	0
11	6	0	23	0	0
12	0	0	24	0	0

3.1. Simulation results

In order to test the algorithm, the load profile depicted in Figure 3 is considered, and the simulation results are run over a full day and night, subjecting the network to each of its three possible load densities. During the first load level, from 0 to 8 hours, the network is experiencing a load equivalent to 0.6 PU. In the second load level, which encompasses levels 8 through 16, the total amount of load increases, reaching 0.9 PU. When you reach the age of 16, you will advance to the third bar level, where you will remain until you reach the age of 24. When comparing this state to the previous one, it is evident that the load has increased to 0.7 PU. In the following sections, the results and analyses for each load level are presented separately.

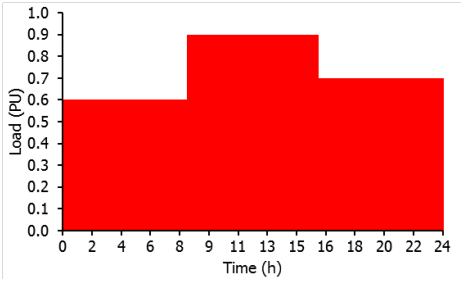

Fig. 4. Load profile for a 24 hour in a day.

3.2. First time level results

The initial time level already contains sixty percent of the total network load. Fig. 5-a depicts the voltages of the first sample bus and the third sample bus in this scenario to be 0.979 and 0.941, respectively. In addition, Fig. 5-b reveals that the power factor is 0.88 after the phase has been completed. The mentioned values fall outside the optimal range specified by the proposed method; consequently, the decision made by the optimized system is necessary to improve the situation. The optimization method concludes that the first bus capacitors should be activated after examining the voltage values of the first bus and the power factor of the PCC bus. Following the activation of the first bus capacitors as depicted in Fig. 7-b, the voltage value of the first bus and the power factor of the PCC bus, which are depicted in Figs. 5-a and 5-a, respectively, become 0.996% and 1.000 PU. This occurs after the initial bus capacitors have been activated.

The voltages on the third bus must fall outside of the desired range for the second control stage to be activated. 5-a reveals that the third buses have respective voltage values of 0.941 PU. Due to the fact that these values are less than the desired value, the second stage is carried out. Adjusting the voltage level of the third bus to correspond with 6 is the initial step. Then, as depicted in 5-a, one of the corresponding feeder capacitors must be activated at fifty percent capacity until the voltage value of the third bus

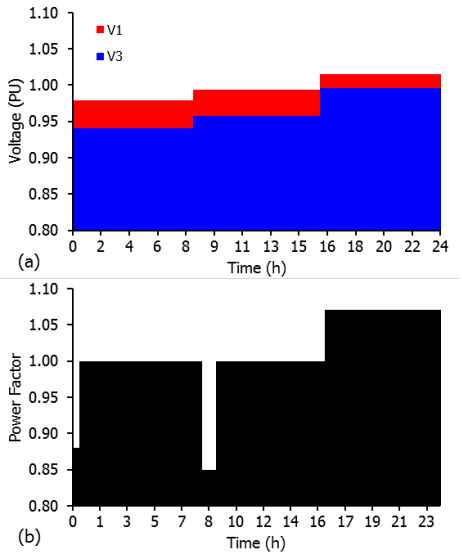

Fig. 5. Simulation results of a) voltage and b) power factor .

reaches 0.958 PU. From the perspective of the phase system, this value is desirable, and the voltage control of the third bus has been completed. The voltage on the first bus must fall outside of the range of 0.95 to 1.05 PU in order to pass the third control stage's requirements. This is a requirement. As illustrated in 5-a, the voltage of the first bus is 0.994, which is the ideal value, and the third control stage is not executed. This configuration yields the best outcome. The voltages of the first and third buses are 0.994 and 0.978, respectively, according to5, and the power factor of the PCC bus is 1.

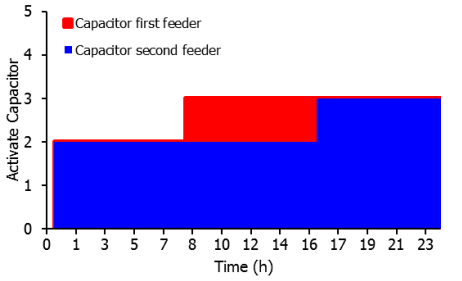

Fig. 6. Simulation results of the number of the active capacitor.

3.3. Second time level results

During the second time period, the load value rises to 0.9 PU, and according to 5, the voltage values of the first and third buses are 0.979 PU and 0.941 PU, respectively. Moreover, the PCC bass power coefficient has reached 0.85 at this time. After an increase of one tap per 5-a, the voltage values of the first and third buses are 0.981 and 0.994, respectively, while the power factor of the PCC bus is 1.00. This occurs during the initial stage of control. The favorable voltage on the first and third buses will prevent the second control stage from being implemented.

3.4. Third time level results

The total fee decreases from 1.0 PU at midnight to 0.7 PU at 16:00. 5 demonstrates that the voltage on the first and third buses reaches 1.016 per unit, whereas the power factor on the PCC bus reaches 1.071 PU. This is the case in the discussed scenario. As each of the specified values corresponds to a desirable result, none of the control steps will be executed.

Table 2. The effect of gas price fluctuations on profit and cost in optimal condition.

Load	0.6 PU		0.9 PU		0.7 PU	
	Current study	[34]	Current study	[34]	Current study	[34]
First bus voltage (PU)	1.037	1.016	1.025	0.994	1.050	0.979
First feeder capacitor	2	3	2	3	2	2
second feeder capacitor	1	3	2	2	1	2

3.5. Validation result

To demonstrate the validation of method, the results of this study are compared with Vargas et al. [34] in Table 1. According to Table 1, it can be seen that in all network load conditions, from the lowest to the highest, the results of this study method has a higher degree of accuracy and the voltage value is set close to one (RMSE=0.85). According to the position of the tap given in Table 1, the tap switching of the transformer in the presented method is less than in the Vargas et al. [34] method demonstrating one of the benefits of the proposed method. In accordance with the number of active feeder capacitors in Table 2, the capacitors are activated in steps with half capacity in this study so that the power factor of the network does not pre-phase and the voltage value of the first bus does not exceed the desired limit.

The results depicted in Fig. 7 illustrate the output of the capacitor voltage transformer, distance voltage, and proposed distance relay for a two-phase fault. The traditional method without optimization was utilized to obtain the distance voltage output, while the optimization algorithm was employed to generate the proposed distance relay output. The observation reveals that the distance relay, in the absence of the optimization algorithm, has triggered the aforementioned error that lies beyond the protection zone and has exceeded the range limit. Conversely, the relay equipped with the suggested algorithm has remained stable at this distance and has not identified any errors.

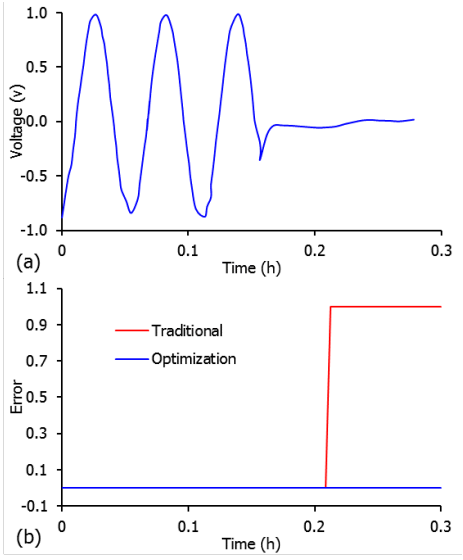

Fig. 7. a) Secondary voltage and distance relay output b) error of different methods.

The optimal form of loss in an electrical system should be between 3 and 6 percent. In developing nations, the proportion of active power losses is approximately 23%. Consequently, minimizing active power losses is crucial for distribution networks. In India, approximately 23% of power was lost across all provinces. To construct a system loss reduction program in the distribution system, it is necessary to reduce power losses using computational tools effectively. Several authors have investigated power losses from various perspectives.

4. CONCLUSIONS

In this study, an optimization model for coordinating the performance of OLTC and CB is investigated. In this method, a structure containing 30 zones is provided, and for each zone, a scenario involving the movement of the tap transformer or capacitor steps is defined. Based on the voltage value, power factor, and proposed structure, the GA algorithm determines a new state for the tap transformer and capacitor. By applying the new state of the control variables (transformer tap and capacitor) to the network, the voltage and power factor improve, and this process is repeated until the voltage and power factor are within the standard parameters. The first advantage of the method is that it increases precision and places the bus voltage and power factor within the allowable range. The second benefit of this method is the automated determination of the new status of the control variables. In order to validate the proposed method, various load variations were simulated. In addition, a comparison between the proposed method and the previous method demonstrates that voltage regulation and power factor correction have been improved. In the proposed method, tap transformer switching is less frequent than in the previous method, reducing costs and extending the transformer's lifespan. The objective of optimizing energy consumption is to select patterns, adopt, and implement methods and policies for the consumption of electric energy. The residential sector is a significant consumer of electric energy. Intelligent management system technology implemented in residential buildings has optimized the consumption of electrical energy to some degree. During the initial load level, which spans from 0 to 8 hours, there exists a network load that is equivalent to 0.6 PU. During the second load level, which encompasses levels 8 to 16, there is a notable increase in the overall load amount, ultimately culminating in a value of 0.9 PU. Upon attaining the age of 16, individuals will transition to the third level of the bar system, where they will remain until reaching the 24 hour. 3–6% electrical system loss is ideal. Distribution networks must minimize active power losses. Computational tools must reduce power losses to build a distribution system loss reduction program. Several authors have studied power losses.

REFERENCES

[1] J. Liu, Z. Zhao, J. Ji, and M. Hu, "Research and application of wireless sensor network technology in power transmission and distribution system," Intell. Converged Networks, vol. 1, no. 2, pp. 199–220, Sep. 2020, doi: 10.23919/ICN.2020.0016.

[2] A. Ardeshiri, A. Lotfi, R. Behkam, A. Moradzadeh, and A. Barzkar, "Introduction and Literature Review of Power System Challenges and Issues," Appl. Mach. learn. Deep learn. Methods Power Syst. Prob., 2021, pp. 19–43. doi: 10.1007/978-3-030-77696-1-2.

[3] Z. Li, W. Jiang, A. Abu-Siada, Z. Li, Y. Xu, and S. Liu, "Research on a Composite Voltage and Current Measurement Device for HVDC Networks," IEEE Trans. Ind. Electron. IEEE, vol. 68, no. 9, pp. 8930–8941, Sep. 2021, doi: 10.1109/TIE.2020.3013772.

[4] L. Schmitz, D. C. Martins, and R. F. Coelho, "Comprehensive Conception of High Step-Up DC–DC Converters With Coupled Inductor and Voltage Multipliers Techniques," IEEE Trans. Circuits Syst. I Regul. Pap., vol. 67, no. 6, pp. 2140–2151, Jun. 2020, doi: 10.1109/TCSI.2020.2973154.

[5] S. Saravanan, P. Usha Rani, and M. P. Thakre, "Evaluation and Improvement of a Transformerless High-Efficiency DC–DC Converter for Renewable Energy Applications Employing a Fuzzy Logic Controller," Mapan - Journal of Metrology Society of India, vol. 37, no. 2, pp. 291–310, 2022, doi: 10.1007/s12647-021-00530-5.

[6] D. Zhao, Y. Cao, D. Gu, S. Zhao, and C. Liu, "Influence of Capacitor Voltage Transformer's Transient Response on Commutation of HVDC Transmission System," in Proceedings of 2020 IEEE Int. Conf. Adv. Electr. Eng. Comput. Appl., AEECA 2020, 2020, pp. 381–388. doi: 10.1109/AEECA49918.2020.9213577.

[7] M. Pourmirasghariyan, S. F. Zarei, and M. Hamzeh, "DC-system grounding: Existing strategies, performance analysis, functional characteristics, technical challenges, and selection criteria - a review," Electric Power Systems Research, vol. 206. 2022. doi: 10.1016/j.epsr.2021.107769.

[8] N. Rezaei and M. N. Uddin, "An Analytical Review on State-of-the-Art Microgrid Protective Relaying and Coordination Techniques," IEEE Trans. Ind. Appl., vol. 57, no. 3. pp. 2258–2273, 2021. doi: 10.1109/TIA.2021.3057308.

[9] P. Tanha Bashoo and M. Jazaeri, "A New Multifunctional Protection System for Reducing Fault Current, Ferroresonance Overvoltage, and Voltage Fluctuations in Power Networks," Int. Trans. Electr. Energy Syst., vol. 2022, pp. 1–19, 2022, doi: 10.1155/2022/1398097.

[10] M. Talebzadeh, A. Setayeshmehr, and H. Barati, "Investigation of Increasing Accuracy Distributed Voltage on the Power Transformer Disks Considering Mutual Induction and Different Grounding System Models," J. Oper. Autom. Power Eng., vol. 10, no. 3, pp. 228–234, 2022, doi: 10.22098/joape.2022.9786.1684.

[11] M. İnci, "A flexible perturb & observe MPPT method to prevent surplus energy for grid-failure conditions of fuel cells," Int. J. Hydrogen Energy, vol. 46, no. 79, pp. 39483–39498, 2021, doi: 10.1016/j.ijhydene.2021.09.185.

[12] B. M. Said, K. D. Eddine, and C. Salim, "Artificial neuron network based faults detection and localization in the high voltage transmission lines with MHO distance relay," J. Eur. Syst. Autom., vol. 53, no. 1, pp. 137–147, 2020, doi: 10.18280/jesa.530117.

[13] M. Koruzhde and Ronald W. Cox, "The Transnational Investment Bloc in U.S. Policy Toward 1. Koruzhde, M.; Ronald W. Cox The Transnational Investment Bloc in U.S. Policy Toward Saudi Arabia and the Persian Gulf. Class, Race and Corporate Power 2022, 10.Saudi Arabia and the Persian Gulf," Cl. Race Corporate Power, vol. 10, no. 1, 2022.

[14] M. Koruzhde and V. Popova, "Americans Still Held Hostage: A Generational Analysis of American Public Opinion About the Iran Nuclear Deal," Polit. Sci. Q., vol. 137, no. 3, pp. 511–537, Sep. 2022, doi: 10.1002/polq.13387.

[15] M. Koruzhde, "The Iranian Crisis of the 1970s-1980s and the Formation of the Transnational Investment Bloc," Cl. Race Corporate Power, vol. 10, no. 2, 2022.

[16] K. R. Dhenuvakonda, A. Singh, M. P. Thakre, R. R. Karasani, and R. Naidoo, "Adaptive digital distance relay for SSSC-based double-circuit transmission line using phasor measurement unit," Int. Trans. Electr. Energy Syst., vol. 29, no. 4, 2019, doi: 10.1002/etep.2787.

[17] F. Aminifar, M. Abedini, T. Amraee, P. Jafarian, M. H. Samimi, and M. Shahidehpour, "A review of power system protection and asset management with machine learning techniques," Energy Syst., vol. 13, no. 4. pp. 855–892, 2022. doi: 10.1007/s12667-021-00448-6.

[18] M. . Gilany, B.-E. Hasan, and O. . Malik, "The Egyptian Electricity Authority strategy for distance relay setting: problems and solutions," Electr. Power Syst. Res., vol. 56, no. 2, pp. 89–94, Nov. 2000, doi: 10.1016/S0378-7796(00)00093-6.

[19] Y. Q. Xia, K. K. Li, and A. K. David, "Adaptive relay setting for stand-alone digital distance protection," IEEE Trans. Power Delivery, vol. 9, no. 1, pp. 480–491, 1994, doi: 10.1109/61.277720.

[20] Zhang Zhizhe and C. Deshu, "An adaptive approach in digital distance protection," IEEE Trans. Power Delivery, vol. 6, no. 1, pp. 135–142, 1991, doi: 10.1109/61.103732.

[21] E. Sorrentino, "Comparison of five methods of compensation

for the ground distance function and assessment of their effect on the resistive reach in quadrilateral characteristics," Int. J. Electr. Power Energy Syst., vol. 61, pp. 440–445, Oct. 2014, doi: 10.1016/j.ijepes.2014.03.049.

[22] A. N. Sarwade, P. K. Katti, and J. G. Ghodekar, "Advanced distance relay characteristics suitable for dynamic loading," Conf. Proc. IPEC, Oct. 2010, pp. 509–514. doi: 10.1109/IPECON.2010.5697049.

[23] M. Kezunovic, L. J. Kojovic, V. Skendzic, C. W. Fromen, D. R. Sevcik, and S. L. Nilsson, "Digital models of coupling capacitor voltage transformers for protective relay transient studies," IEEE Trans. Power Delivery, vol. 7, no. 4, pp. 1927–1935, 1992, doi: 10.1109/61.156996.

[24] D. Hou and J. Roberts, "Capacitive voltage transformer: transient overreach concerns and solutions for distance relaying," Can. Conf. Electr. Comput. Eng., 1996, vol. 1, pp. 119–125. doi: 10.1109/ccece.1996.548052.

[25] H. B. Siguerdidjane, J. Gaonach, and N. Le Rohellec, "Applications of digital power simulators: Advantages," IEEE Trans. Power Delivery, vol. 12, no. 3, pp. 1137–1141, 1997, doi: 10.1109/61.636921.

[26] H. Khorashadi-Zadeh, "Correction of capacitive voltage transformer distorted secondary voltages using artificial neural networks," Semin. Neural Network appl. Electr. Eng. Proc., NEUREL 2004, 2004, pp. 131–134. doi: 10.1109/neurel.2004.1416555.

[27] H. Yousefi, S. A. Gholamian, and A. Zakariazadeh, "Distributed voltage control in distribution networks with high penetration of photovoltaic systems," J. Oper. Autom. Power Eng., vol. 8, no. 2, pp. 164–171, 2020, doi: 10.22098/joape.2020.6259.1472.

[28] S. Il Go, S. Y. Yun, S. J. Ahn, and J. H. Choi, "Voltage and Reactive Power Optimization Using a Simplified Linear Equations at Distribution Networks with DG," Energ., vol. 13, no. 13, 2020, doi: 10.3390/en13133334.

[29] Z. Rui, L. Jifeng, L. Kecheng, L. Anchang, L. Xiaoming, and G. Jianhu, "The Optimization for Voltage and Reactive Power Control of Distribution Network Considering Equipment Operation Loss," IEEE/IAS Ind. Commer. Power Syst. Asia (I&CPS Asia), Jul. 2021, pp. 965–969. doi: 10.1109/ICPSAsia52756.2021.9621667.

[30] X. Huang, G. Zu, Q. Ding, R. Wei, Y. Wang, and W. Wei, "An Online Control Method of Reactive Power and Voltage Based on Mechanism–Data Hybrid Drive Model Considering Source–Load Uncertainty," Energ., vol. 16, no. 8, p. 3501, Apr. 2023, doi: 10.3390/en16083501.

[31] A. Pouladi, A. K. Zadeh, and A. Nouri, "Control of Parallel ULTC Transformers in Active Distribution Systems," IEEE Syst. J., vol. 14, no. 1, pp. 960–970, 2020, doi: 10.1109/JSYST.2019.2897771.

[32] P. Singh, S. K. Bishnoi, and N. K. Meena, "Moth Search Optimization for Optimal DERs Integration in Conjunction to OLTC Tap Operations in Distribution Systems," IEEE Syst. J., vol. 14, no. 1, pp. 880–888, 2020, doi: 10.1109/JSYST.2019.2911534.

[33] S. Magnússon, G. Qu, and N. Li, "Distributed Optimal Voltage Control with Asynchronous and Delayed Communication," IEEE Trans. Smart Grid, vol. 11, no. 4, pp. 3469–3482, 2020, doi: 10.1109/TSG.2020.2970768.

[34] R. Vargas, L. H. MacEdo, J. M. Home-Ortiz, J. R. S. Mantovani, and R. Romero, "Optimal Restoration of Active Distribution Systems with Voltage Control and Closed-Loop Operation," IEEE Trans. Smart Grid, vol. 12, no. 3, pp. 2295–2306, 2021, doi: 10.1109/TSG.2021.3050931.

[35] F. Xu, Q. Guo, H. Sun, B. Zhang, and L. Jia, "A two-level hierarchical discrete-device control method for power networks with integrated wind farms," J. Mod. Power Syst. Clean Energy, 2019, doi: 10.1007/s40565-018-0417-1.

[36] K. K. Mehmood, S. U. Khan, S.-J. Lee, Z. M. Haider, M. K. Rafique, and C.-H. Kim, "A real-time optimal coordination scheme for the voltage regulation of a distribution network including an OLTC, capacitor banks, and multiple distributed energy resources," Int. J. Electr. Power Energy Syst., vol. 94, pp. 1–14, Jan. 2018, doi: 10.1016/j.ijepes.2017.06.024.

[37] K. Alzaareer, M. Saad, H. Mehrjerdi, D. Asber, and S. Lefebvre, "Development of New Identification Method for Global Group of Controls for Online Coordinated Voltage Control in Active Distribution Networks," IEEE Trans. Smart Grid, vol. 11, no. 5, pp. 3921–3931, Sep. 2020, doi: 10.1109/TSG.2020.2981145.

[38] S. Riahinia, A. Abbaspour, M. Moeini-Aghtaie, and S. Khalili, "Load service restoration in active distribution network based on stochastic approach," IET Gener. Transm. Distrib., vol. 12, no. 12, pp. 3028–3036, Jul. 2018, doi: 10.1049/iet-gtd.2017.0684.

[39] D. S. Sanches, J. B. A. London Junior, and A. C. B. Delbem, "Multi-Objective Evolutionary Algorithm for single and multiple fault service restoration in large-scale distribution systems," Electr. Power Syst. Res., vol. 110, pp. 144–153, May 2014, doi: 10.1016/j.epsr.2014.01.017.

[40] L. T. Marques, A. C. B. Delbem, and J. B. London, "Service Restoration with Prioritization of Customers and Switches and Determination of Switching Sequence," IEEE Trans. Smart Grid, pp. 1–1, 2017, doi: 10.1109/TSG.2017.2675344.

[41] S. Li and D. Li, "Genetic Algorithms," in Springer Series in Materials Science, vol. 312, 2021, pp. 115–131. doi: 10.1007/978-3-030-68310-8-5.

[42] I. Delyová et al., "Sizing and topology optimization of trusses using genetic algorithm," Mater., vol. 14, no. 4, pp. 1–14, 2021, doi: 10.3390/ma14040715.